Local force constants of transition metal dopants in a nickel host: Comparison to Mossbauer studies

M. Daniel,[1] D. M. Pease,[2] N. Van Hung,[3] and J. I. Budnick[2]
[1]*Physics Department, University of Nevada, Las Vegas, Nevada 89154, USA*
[2]*Physics Department, University of Connecticut, Storrs, Connecticut 06269, USA*
[3]*University of Science, Vietnam National University-Hanoi, Hanoi, Vietnam*
(Received 22 August 2003; revised manuscript received 8 January 2004; published 12 April 2004)

We have used the x-ray absorption fine-structure technique to obtain temperature-dependent mean-squared relative displacements for a series of dopant atoms in a nickel host. We have studied the series Ti, V, Mn, Fe, Nb, Mo, Ru, Rh, and Pd doped into Ni, and have also obtained such data for pure Ni. The data, if interpreted in terms of the correlated Einstein model of Hung and Rehr, yield a ratio of a (host-host) to (host-impurity) effective force constant, where the effective force constant is due to a cluster of atoms. We have modified the method of Hung and Rehr so that we obtain a ratio of near-neighbor single spring constants, rather than effective spring constants. We find that the host to the $4d$ impurity force constant ratio decreases monotonically as one increases the dopant atomic number for the series Nb, Mo, Ru, and Rh, but after a minimum at Rh the ratio increases sharply for Pd. We have compared our data to Mossbauer results for Fe dopants in Ni, and find qualitative disagreement. In Mossbauer studies, the ratio of the Ni-Ni to Fe-Ni force constant is found to be extremely temperature dependent and less than one. We find the corresponding ratio, as interpreted in terms of x-ray absorption spectra and the correlated Einstein model, to be greater than one, a result that is supported by elastic constant measurements on $Ni_xFe_{(1-x)}$ alloys.

DOI: 10.1103/PhysRevB.69.134414 PACS number(s): 75.30.Hx

I. INTRODUCTION

It would be of interest if a general method existed for determining local force constants for dopants in dilute binary alloys. For instance, force constants can be of use in constructing local atomic potentials used in simulations.[1] The Mössbauer effect has been used extensively to measure the ratio r_X of host-host to impurity-host local force constants for dilute alloys,[2] but is limited to cases for which the dopant atomic species is Mossbauer active. X-ray absorption fine structure (XAFS) can also be related to local force constant ratios, and unlike the Mossbauer effect can be applied to a wide variety of atomic types. The Mossbauer measurements can be interpreted in terms of force constants using an analytic result due to Mannheim that is exact, assuming central, near-neighbor forces and a cubic host matrix.[3] Temperature-dependent x-ray extended fine-structure results can be related to local force constants using the correlated Einstein model of Hung and Rehr;[4] this is a simplified approach that considers a single pair of vibrating atoms in a small cluster and assumes a Morse potential. As in the Mossbauer theory of Mannheim, central forces are assumed. Despite these approximations, the correlated Einstein model does yield a curve of mean-square relative displacement versus temperature that is in good agreement with experiment for pure copper metal. We note that for several pure fcc metals, Daniel *et al.* have shown that the slope of the linear portion of a plot of temperature versus XAFS-derived mean-squared relative displacement (MSRD) may be expected to be approximately proportional to a bulk shear modulus.[5] These authors also showed this relationship to be true experimentally. In the present study we analyze temperature-dependent XAFS data to obtain the ratio of pure host to dopant-host single spring force constants for an impurity atom in a fcc host matrix We use an augmented version of the correlated Einstein model of Van Hung and Rehr. We find that for the $4d$ impurities in Ni there is a monotonic decrease in force constant ratio as one increases the dopant atomic number in going along the series Nb, Mo, Ru, and Rh. However, for the case of Pd dopants the force constant ratio increases sharply relative to the case of Rh dopants. These results are interpreted in terms of theories of size difference—shear modulus relationships, as well as the known shear moduli of the pure fcc metals Rh and Pd. Finally, we compare Mossbauer and XAFS results for the host to impurity atom force constant ratio for Fe dopants in Ni.

We have made an experimental determination of the absorber–near-neighbor mean-squared relative displacement (MSRD) versus temperature for a systematic series of impurity atoms in a nickel matrix. We performed experiments on $3d$ dopants from Ti through Fe, alloyed into Ni, and on $4d$ dopants from Nb through Pd also alloyed into Ni. In the present work we consider the MSRD between the dopant, whose absorption edge is measured, and the near-neighbor host atom. The MSRD is related to the mean-squared displacement (MSD) by the following relationship:

$$\mathrm{MSRD} = \mathrm{MSD}_{\mathrm{IMPURITY}} + \mathrm{MSD}_{\mathrm{NN\ HOST}} - 2(\mathrm{DCF}). \quad (1)$$

In the above, the DCF refers to the displacement correlation function (DCF) as discussed, for instance, by Beni and Platzman.[6] Recently, Poiarkova and Rehr have developed a method for numerical computation of the MSRD for assumed local force constants.[7] This method is not yet available for the general user. At present the best theoretical framework with which the experimentalist can relate force

constants to temperature-dependent XAFS is the correlated Einstein model.[4]

II. DISCUSSION OF THE CORRELATED EINSTEIN MODEL: THEORETICAL BACKGROUND

Van Hung and Rehr use their correlated Einstein model to compute an effective force constant for an absorbing atom in a small cluster of host atoms. The cluster consists of the absorber (impurity) atom, host near neighbors of the absorber atom, and host near neighbors of the near neighbors of the impurity atom.[4] The effective force constant relates to the normal mode for which the impurity atom (I) and one near neighbor (NN) vibrate back and forth about the common center of mass of the I and NN pair. In this model, all other atoms are assumed fixed in place. In the present application we assume an impurity atom doped into a fcc host lattice. The calculated effective spring constant k_{EFF} is related to an effective potential $V_E(x)$ by Eq. (2),

$$V_E(x) \sim (1/2)k_{\mathrm{EFF}}x^2 + k_3x^3 + \cdots, \tag{2}$$

where the ellipses indicate higher order terms. In Eq. (2), x is the deviation, from the equilibrium separation, of the bond length between the two atoms vibrating in this normal mode as *both* atoms move relative to their common center of mass, and k_3 is a cubic anharmonicity parameter. For the fcc lattice, the motion of the two atoms in question is along the [110] direction. The present study uses a range of temperatures such that terms of higher order than quadratic in x are negligible. The model of Van Hung and Rehr assumes central forces only, and assumes that only near-neighbor forces are significant.

We wish to relate our work to existing Mossbauer results. The Mossbauer theory of Mannheim also assumes the validity of near-neighbor central forces and the harmonic approximation.[3] The Mossbauer results are expressed in terms of a spring constant (restoring force per unit displacement) that is defined as if *only* the impurity atom were moved along an *arbitrary* x direction, all other atoms fixed, and the restoring force is also along x. The constant $A_{XX}(0,0)$ for the pure host equals four times the single spring constant between a particular pair of near-neighbor atoms. For a substitutional impurity atom at the origin, we define $A_{xx\ \mathrm{IMPURITY}}(0,0)$ as the restoring force in the x direction per unit displacement in the x direction of the impurity atom at the origin, holding all other atoms fixed. Then $A_{xx\ \mathrm{IMPURITY}}(0,0)$ is shown by Mannheim to be equal to four times the single spring constant between the impurity atom and a near-neighbor host atom. We define the single spring force constant between the impurity atom and the host atom, where the direction from the impurity to the host atom is [110], to be k_{HI}. We define the corresponding single spring force constant between an atom in the pure host lattice and a near-neighbor host atom, to be k_{HH}. These quantities are to be determined from XAFS. Then one has the relationships as shown in Eq. (3),

$$A_{XX}(0,0) = 4k_{HH}, \quad A_{XX\ \mathrm{IMPURITY}}(0,0) = 4k_{HI}. \tag{3}$$

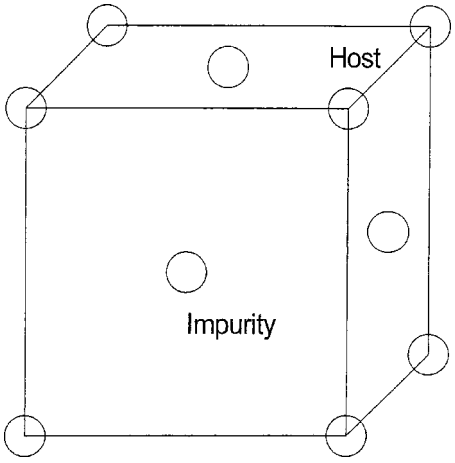

FIG. 1. Schematic drawing of the cluster used in the correlated Einstein model of Hung and Rehr.

We define the ratio r_X to be equal to k_{HH} divided by k_{HI}. Given the definitions outlined above it is clear that the ratio r_X to be determined from the XAFS analysis is equal to the ratio λ determined from Mossbauer experiments, as written in Eq. (4),

$$r_X = k_{HH}/k_{HI} = A_{XX}(0,0)/A_{XX\ \mathrm{IMPURITY}}(0,0) = \lambda. \tag{4}$$

The effective force constant between the impurity atom and a near-neighbor host atom, in the atomic cluster used in the correlated Einstein model, is defined as k_{EFF}. The effective spring constant between neighboring atoms in a pure host lattice is denoted by $k_{\mathrm{PURE\ EFF}}$. Our first task is to obtain a relationship that will enable us to determine k_{HI} and k_{HH} in terms of k_{EFF} and $k_{\mathrm{PURE\ EFF}}$ and relate the XAFS data to a quantity involving the spring constant ratio r_X. In Fig. 1 we illustrate a section of the three-dimensional cluster used to discuss our derivation. Let x_I be a displacement of the impurity atom along the [110] axis toward the host atom. Let x_H be a displacement of the host atom along this same axis toward the impurity atom. All other atoms are fixed. These displacements are assumed to correspond to the normal-mode described above and, therefore, one has the relationship described in Eq. (5),

$$(x_I/x_H) = (M_H/M_I). \tag{5}$$

In the above equation, M_H and M_I are the masses of the host and impurity atom, respectively. Then, in a straightforward but somewhat tedious and lengthy application of classical mechanics, we consider all out of plane and in plane force contributions and keep only quadratic contributions to all potentials. The total increase in potential of the I and H atoms due to a total change of amount x in near-neighbor bond length is then given by Eq. (6),

$$V_E(x) = \tfrac{1}{2}\{k_{HI}(x^2 - x_I^2) + 3k_{HH}x_H^2 + 4k_{HI}x_I^2\}. \tag{6}$$

In the derivation of Eq. (6) it is assumed that the atomic displacements are sufficiently small relative to the interatomic distances involved that the angle between the displacement of an atom and the directional vector to a particu-

lar near-neighbor atom does not change during that displacement. The effective spring constant can then be expressed in terms of single spring constants as in Eq. (7),

$$k_{\mathrm{EFF}}=3k_{HH}[M_I/(M_H+M_I)]^2+4k_{HI}[M_H/(M_H+M_I)]^2 + k_{HI}\{1-[M_H/(M_H+M_I)]^2\}. \quad (7)$$

For the case of a pure material, $M_H=M_I$ and $k_{HH}=k_{HI}$, and one obtains an effective pure host spring constant that is 2.5 times the pure host single spring constant. This result agrees with the corresponding result of Van Hung and Rehr for a pure material, obtained by those authors using a Morse potential.[4] For the case in which the ratio of M_H divided by M_I approaches infinity, k_{EFF} approaches $4k_{HI}$. This corresponds to the case in which the host atoms are motionless, and the effective spring constant acting on the impurity is four times the near-neighbor single spring constant k_{HI}, in agreement with Eq. (3). For the case in which the ratio of M_I divided by M_H approaches infinity, k_{EFF} approaches $k_{HI}+3k_{HH}$.

We express our *experimental* XAFS results in terms of a ratio R_X given by Eq. (8), thus utilizing the correlated Einstein model of Van Hung and Rehr,

$$R_X=k_{\mathrm{PURE\ EFF}}/k_{\mathrm{EFF}}. \quad (8)$$

We desire the ratio of near-neighbor single spring force constants r_X, a ratio that must be obtained from the experimental ratio R_X, analyzed by the theory of Van Hung and Rehr.[4] The ratio r_X, determined from XAFS, corresponds to the ratio as determined by the Mossbauer measurements.

We define the constants C_1 and C_2 as follows:

$$C_1=[M_I/(M_H+M_I)]^2, \quad (9)$$

$$C_2=[M_H/(M_I+M_H)]^2. \quad (10)$$

Then one obtains the single spring constant ratio r_X in terms of the experimental ratio R_X as expressed in Eq. (11),

$$r_X=2R_X(3C_2+1)/(5-6C_1R_X). \quad (11)$$

We consider some more limiting cases: (1) For the case in which R_X equals 1, and both atoms have the same mass, r_X also equals 1. (2) In the limit for which M_H/M_I goes to infinity (heavy host atom) R_X approaches $0.625r_X$. One can see that this last result is physically consistent with both the model of Hung and Rehr and the definition of $A_{XX\ \mathrm{IMPURITY}}(0,0)$ used in Mannheim's theory. The value of $k_{\mathrm{PURE\ EFF}}$ equals $2.5k_{HH}$. On the other hand, if the ratio M_H/M_I approaches infinity, then k_{EFF} approaches $A_{XX\ \mathrm{IMPURITY}}(0,0)$ since now only the impurity atom moves. Recall that $A_{XX\ \mathrm{IMPURITY}}=4k_{HI}$. Then the ratio R_X should indeed approach (2.5/4) times r_X, or 0.625 times r_X.

Hung and Rehr find that classical approximations, such as the equipartition of the energy theorem, are valid for temperatures at or above the effective Einstein temperature,[4] which Sevillano *et al.* find to be about 2/3 the Debye temperature for fcc metals.[8] Room temperature is close to two-thirds the Debye temperature for Ni metal. Thus, the conclusions of Sevillano *et al.* applied to our experiments indicate that our data extend into a temperature region for which the MSRD is proportional to temperature and the equipartition of energy theorem can be applied. In a later section of this paper we will justify the assumption that for our data we can neglect the anharmonic terms in Eq. (2). Assuming the validity of Eq. (2), but neglecting anharmonic terms, one has from the equipartition of energy theorem Eq. (12),

$$\tfrac{1}{2}k_{\mathrm{EFF}}\mathrm{MSRD}_{\mathrm{HOST\text{-}IMPURITY}}=\tfrac{1}{2}k_{\mathrm{BOLTZMANN}}T, \quad (12)$$

whereas for a pure host one has Eq. (13), again using the harmonic approximation,

$$\tfrac{1}{2}k_{\mathrm{PURE\ EFF}}\mathrm{MSRD}_{\mathrm{HOST\text{-}HOST}}=\tfrac{1}{2}k_{\mathrm{BOLTZMANN}}T. \quad (13)$$

In an Einstein model, Knapp *et al.* approximate $\mathrm{MSRD}_{\mathrm{HOST\text{-}IMPURITY}}$ by the expression (14),[9]

$$\mathrm{MSRD}_{\mathrm{HOST\text{-}IMPURITY}} = (\hbar/2\mu\omega_{E\ H\text{-}I})\coth[\hbar\omega_{E\ H\text{-}I}/2k_{\mathrm{BOLTZMANN}}T], \quad (14)$$

where μ is the effective mass of the impurity-host pair. For the case of $\mathrm{MSRD}_{\mathrm{HOST\text{-}HOST}}$ one replaces 2μ in Eq. (14) by M_H. The Einstein temperature Θ_E is proportional to the Einstein frequency ω_E. From Eqs. (12) and (13), one obtains Eq. (15), assuming the classical temperature regime and the harmonic approximation,

$$R_X=[dT/d(\mathrm{MSRD}_{\mathrm{HOST\text{-}HOST}})]/[dT/d(\mathrm{MSRD}_{\mathrm{HOST\text{-}IMPURITY}})]. \quad (15)$$

In the high-temperature limit $\coth[\hbar\omega_{E\,H\text{-}I}/2k_{\mathrm{BOLTZMANN}}T]$ approaches $2k_{\mathrm{BOLTZMANN}}T/\hbar\omega_{E\ H\text{-}I}$. Also $\coth[\hbar\omega_E/2k_{\mathrm{BOLTZMANN}}T]$ approaches $2k_{\mathrm{BOLTZMANN}}T/\hbar\omega_{E\ \mathrm{HOST}}$ and one has

$$R_X=[\Theta_{E\ \mathrm{HOST}}/\Theta_{E\ H\text{-}I}]^2M_H/2\mu. \quad (16)$$

Finally, combining Eqs. (11) and (16), one has the desired result expressed in Eq. (17),

$$r_X=2[\Theta_{E\ \mathrm{HOST}}/\Theta_{E\ H\text{-}I}]^2(M_H/2\mu)(3C_2+1)/\{5 - 6C_1[\Theta_{E\ \mathrm{HOST}}/\Theta_{E\ H\text{-}I}]^2(M_H/2\mu)\}. \quad (17)$$

We now show that we can neglect anharmonic terms in Eq. (2) for our experiments performed for temperatures less than 300 °C on Ni-based alloys. Hung *et al.* have recently performed a detailed analysis of the anharmonic contributions to the XAFS for copper metal.[10] They find that, in terms of the MSRD, ''the difference between the total and harmonic values becomes visible at 100 K, but it is very small and can be important only from about room temperature.'' In the high-temperature limit, for the correlated Einstein model, the MSRD between near neighbors is given by the expression[4]

$$\mathrm{MSRD}=k_{\mathrm{BOLTZMANN}}T/5D\alpha^2, \quad (18)$$

where D and α are parameters characterizing a Morse potential local to the pure host atom in the host matrix. In the paper by Hung and Rehr,[4] the effective spring constant, for a pure fcc material, is related to the Morse potential as follows:

$$K_{(\text{EFF PURE HOST})} = 5D\alpha^2[1-(3/2)\alpha a], \tag{19}$$

where "a" is a net thermal expansion. From Girafalco and Weizer,[11] α for Ni is 1.42 Å^{-1}. The nearest-neighbor distance in the fcc Ni lattice is close to 2.5 Å. From the known value of the thermal expansion coefficient of Ni metal[12] of 12.5 $\times 10^{-6}$, one deduces that to a very good approximation, at room temperature, one can neglect the second term in the parentheses in the right side of Eq. (19). We note that the thermal expansion coefficients of Ni, Ti, V, Cr, Fe, Nb, Mo, Ru, Rh, and Pd are all less than Cu.[13] One would therefore expect the statement of Hung *et al.* that the anharmonic terms are unimportant up to room temperature for Cu (Ref. 10) to hold *a fortiori* for Ni-based alloys with small amounts of these dopants. (The listed thermal expansion coefficient of pure Mn exceeds that of copper. In pure form, this material has a large, complex unit cell relative to the other metals listed, and therefore the large thermal expansion for pure Mn is not characteristic of Mn in a fcc environment.)

It is relevant here to discuss again the high-temperature results of Mannheim as applied to a determination of a ratio λ of the host-host to impurity-host force constant[2,3] using Mossbauer data. The theory of Mannheim, for the MSD, and the correlated Einstein model of Hung and Rehr, for the MSRD, are similar in that both assume central forces and a cubic lattice. The theory of Mannheim assumes a harmonic approximation, and relates experimental data and the properties of the host phonon density of states to the ratio given in Eq. (4). Mannheim's theory has been simplified by Grow *et al.* Grow *et al.* show that one obtains the following relationship in the high-temperature limit:[2]

$$\text{MSD} \sim (k_B T/M)\mu(-2). \tag{20}$$

In the above equation, k_B is Boltzmann's constant, M is the mass of the vibrating atom, and $\mu(-2)$ is a moment expansion. By manipulating an expression developed by Grow *et al.*, one can show that in the high-temperature limit one obtains the following equation:

$$\lambda = r_X = 1 + (\beta_{-2})\{[\mu(-2)_{\text{IMPURITY}}/\mu(-2)_{\text{HOST}}] \times (M_H/M_I) - 1\}, \tag{21}$$

where (β_{-2}) is a function of the host phonon density of states. By combining Eqs. (20) and (21) one obtains the following relationship for r_X:

$$r_X \sim 1 + \beta_{-2}[\{(\Delta\text{MSD}_{\text{IMPURITY}}/\Delta T)/(\Delta\text{MSD}_{\text{HOST}}/\Delta T)\} - 1]. \tag{22}$$

In an Einstein model, β_{-2} becomes unity[2] and r_X is equal to the ratio of the high temperature slope of the impurity MSD versus temperature plot, divided by the high temperature slope of the host MSD versus temperature plot. In an Einstein model; therefore, Eq. (22) reduces to the analogous expression as is obtained in Eq. (15) for the quantity R_X, where R_X is equal to the ratio of slopes involving the MSRDs.

III. EXPERIMENTAL METHODS

A. Sample preparation

Dilute samples of $\text{Ni}_{(1-x)}\text{TM}_x$ (TM = Ti, V, Cr, Mn, Fe, Nb, Mo, Ru, Rh, and Pd where $x = 0.01$ or 0.02) were made by melting in an arc melter with Ar back fill. The dopant concentrations used were 1% for Ti, V, Cr, Mn, and Rh dopants and 2% for Fe, Nb, Mo, Ru, and Pd dopants. Several remelts were made to assist in obtaining homogenous ingots. To ensure minimal weight loss the samples were weighed before and after melting. The recovery turned out to be 99.8% or better. The samples were given a homogenization anneal at 800 C for ~100 h. Investigations by x-ray diffraction revealed only fcc Ni peaks.

B. Data collection

The samples were mounted in a "displex" refrigerator system. Using conventional fluorescence geometry, *K*-edge dopant atom XAFS was collected at five different temperatures for each sample. The fluorescence signal from each sample was monitored using an ion chamber filled with either argon or krypton gas. In order to minimize harmonic contamination, the monochromator was detuned by about 40% for $3d$ dopants. For the $4d$ dopants, there was no need for detuning due to the higher energy at which these data were collected. Data were obtained out to 1200 eV above threshold. The data were collected at the X-11A synchrotron line at the National Synchrotron Light Source (NSLS). A double crystal Si(111) monochromator was used.

We also obtained similar temperature-dependent XAFS data for pure Ni, except the Ni data were taken in transmission so as to avoid the distortion effects that arise if fluorescence XAFS is obtained on concentrated specimens. We analyzed the pure Ni data in the manner to be described below, and obtained by our procedures the high-temperature slope of the linear region of a plot of T versus MSRD. In a previous publication we have showed that one would expect such a slope to be a linear function of the bulk shear modulus for pure fcc materials, and then demonstrated that this was indeed the case for a significant set of XAFS data in the literature.[5] Our Ni data point fits quite well on this linear plot. These results show the consistency of the XAFS method, as applied here, between different investigators. Our results for pure Ni also support the soundness of experimental and data analysis techniques used for our present measurements for the alloys of doped TM's in a Ni host. Other evidence supporting the soundness of our procedures may be found in our results for dopant–near-neighbor distances as discussed in following sections.

C. Data analysis

Data was reduced by using the University of Washington XAFS analysis package. The edge energy was chosen at the edge inflection point. When one uses gas-filled ion chambers this produces an energy variation in fluorescence radiation detection efficiency. We corrected for this effect and then the XAFS was isolated from the background by subtracting a cubic polynomial spline. The unweighted XAFS for various

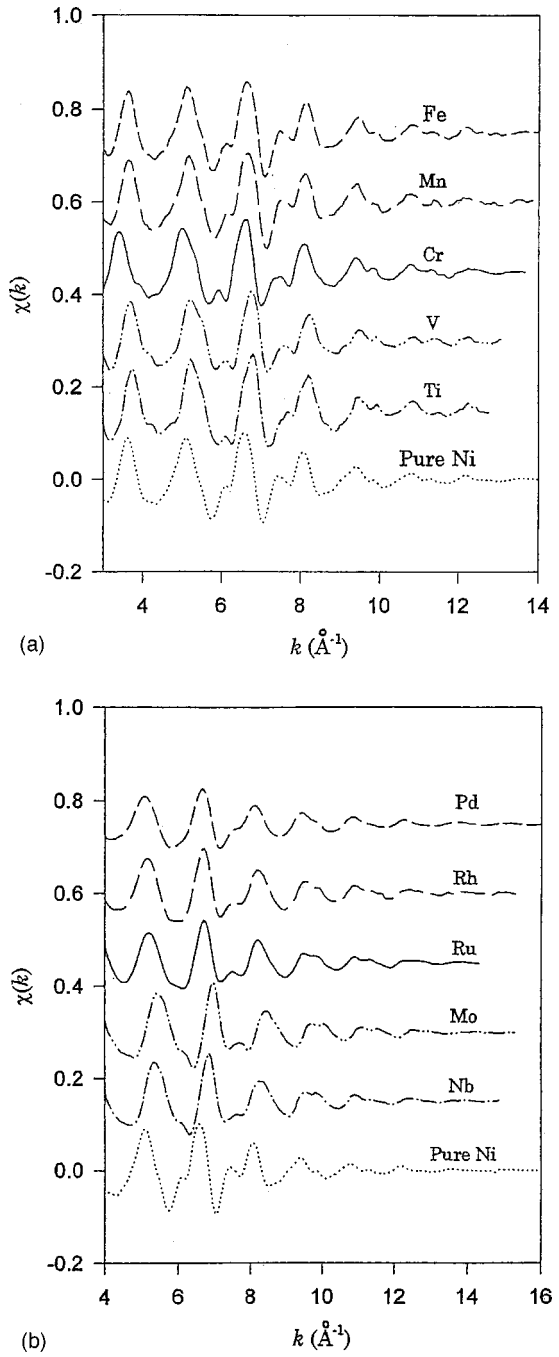

FIG. 2. XAFS $\chi(k)$ function at various (a) $3d$ dopant K edges and (b) $4d$ dopant K edges, taken at room temperature.

$3d$ and $4d$ dopants in Ni obtained at room temperature (300 K) is shown in Figs. 2(a) and 2(b). For comparison, the unweighted XAFS of Ni foil is also displayed at the bottom of each figure. Using FEFFIT, data were fit to theoretical standards generated by FEFF6.[14,15] Data were fit by assuming a fcc Ni near-neighbor environment with the coordination number fixed to 12. The inner potential shift ΔE_0, the many-body amplitude reduction factor S_0^2, and the coordination shell distance were allowed to vary but were constrained to be the same at all temperatures. Fourier transforms obtained for the cases of V and Nb dopants for different temperatures

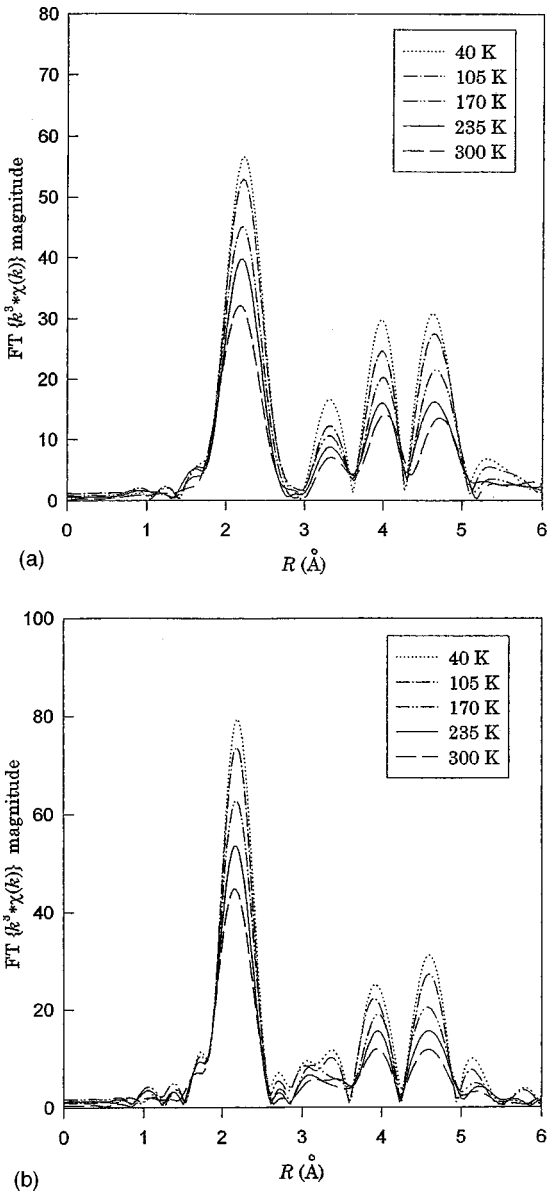

FIG. 3. k^3-weighted Fourier transform for (a) V K-edge XAFS in V_1Ni_{99} and (b) K-edge XAFS in Mo_2Ni_{98}, taken at various temperatures.

are shown in Figs. 3(a) and 3(b). Real parts of these Fourier transforms and fits for the first shell are shown in Figs. 4(a) and 4(b). The differences between the coordination shell distances and the near-neighbor distance in pure Ni, as determined from our fits, were compared to the data of Scheuer *et al.*[16] The trends of our interatomic distances as a function of dopant atom atomic number are in good agreement with the previous results of Scheuer *et al.* The MSRD's for each temperature were allowed to vary and the best MSRD's are extracted from our fits. The difference Δ MSRD between the MSRD values at temperature T and the best value at 40 K are plotted versus temperature for temperatures up to ~300 K. These results are shown in Figs. 5(a) and 5(b). The error bars on individual MSRD points were generated by FEFF6. The Einstein temperatures were obtained by fitting the Δ MSRD plots to Eq. (23),

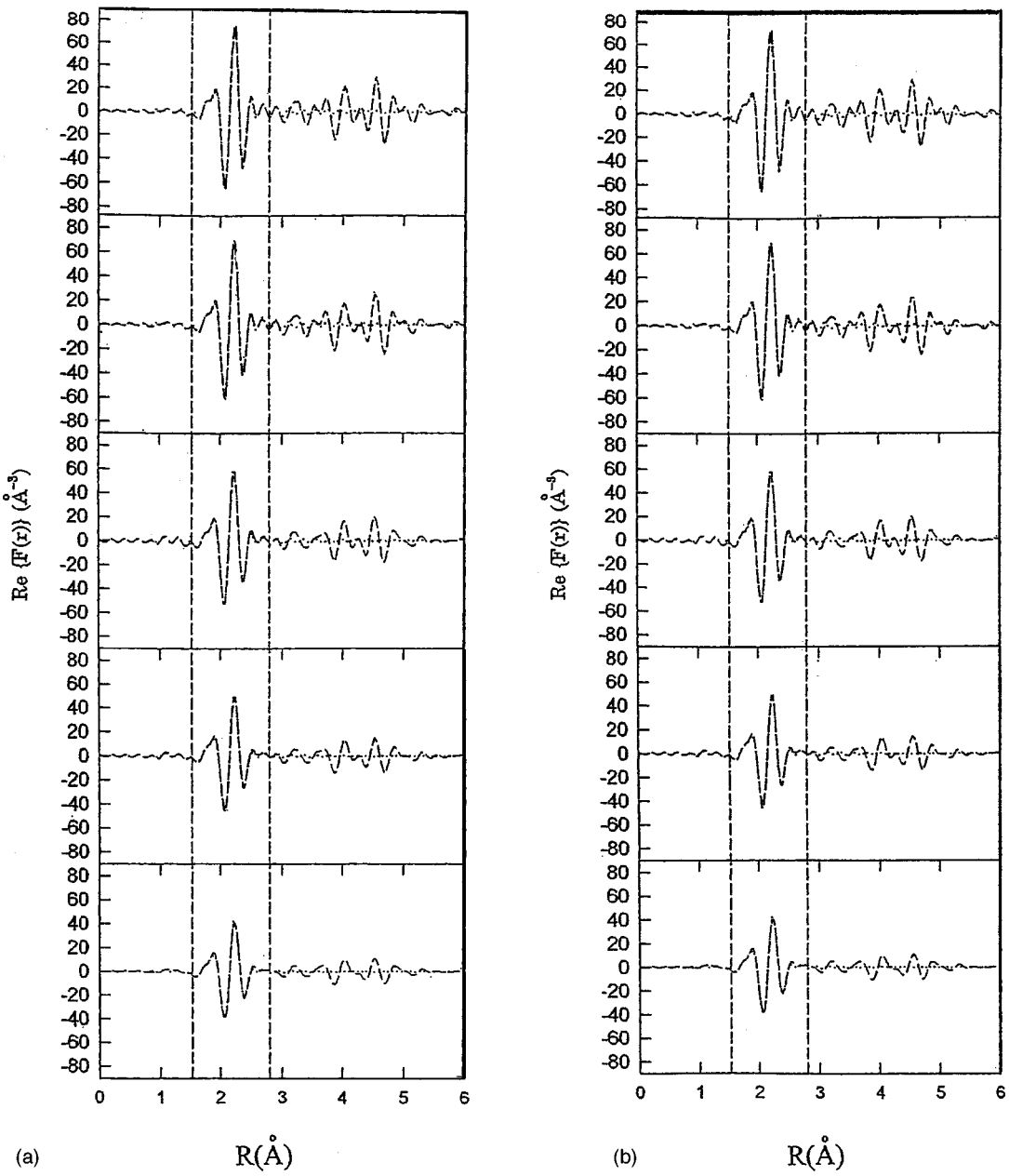

FIG. 4. (a) Real part of the Fourier transformed (k^3-weighted) XAFS data and fit for V_1Ni_{99}. Transform range is 2.49–12.8 A^{-1}. The fit range, 1.41–2.91 A, is indicated by the dashed vertical lines. Temperatures correspond to Fig. 3(a) and are from top to bottom 40, 105, 170, 235, and 300 K. (b) Real part of the Fourier transformed (k^3-weighted) XAFS data and fit for Mo_2Ni_{98}. Transform range is 3.0–15 A^{-1}. The fit range, 1.53–2.82 A, is indicated by the vertical dashed lines. Temperatures correspond to Fig. 3(b) and are from top to bottom 40, 105, 170, 235, and 300 K.

$$\Delta\mathrm{MSRD}_{\mathrm{HOST\text{-}IMPURITY}} = (\hbar^2/2\mu k\Phi_{E\,H\text{-}I})[(\coth\Phi_{E\,H\text{-}I}/2T) - (\coth\Phi_{E\,H\text{-}I}/80)]. \quad (23)$$

On the plots of experimental ΔMSRD versus T points we show the best fit Einstein temperature, an error bar on the Einstein temperature that represents plus or minus twice the standard error for the fit of Eq. (23) to the data points, and a solid line representing a plot of a theoretical ΔMSRD versus T curve resulting from plotting Eq. (23) using the best-fit value of the Einstein temperature. Although the system consisting of Cr doped into Ni was part of our investigation, in this case the error bar for the best-fit Einstein temperature was quite large, and the plot of ΔMSRD points versus T did not show the shape predicted by Eq. (23). Perhaps there is some temperature-dependent effect specific to Cr dopants in Ni that is showing up; however, as far as this particular study is concerned the Cr in Ni data is not shown in Figs. 5(a) and 5(b) nor analyzed further.

The force constant ratios were extracted from the data as described in a previous section, using Eq. (17). Our plots of force constant versus atomic number are displayed in Figs. 6(a) and 6(b). These error bars are computed by starting with

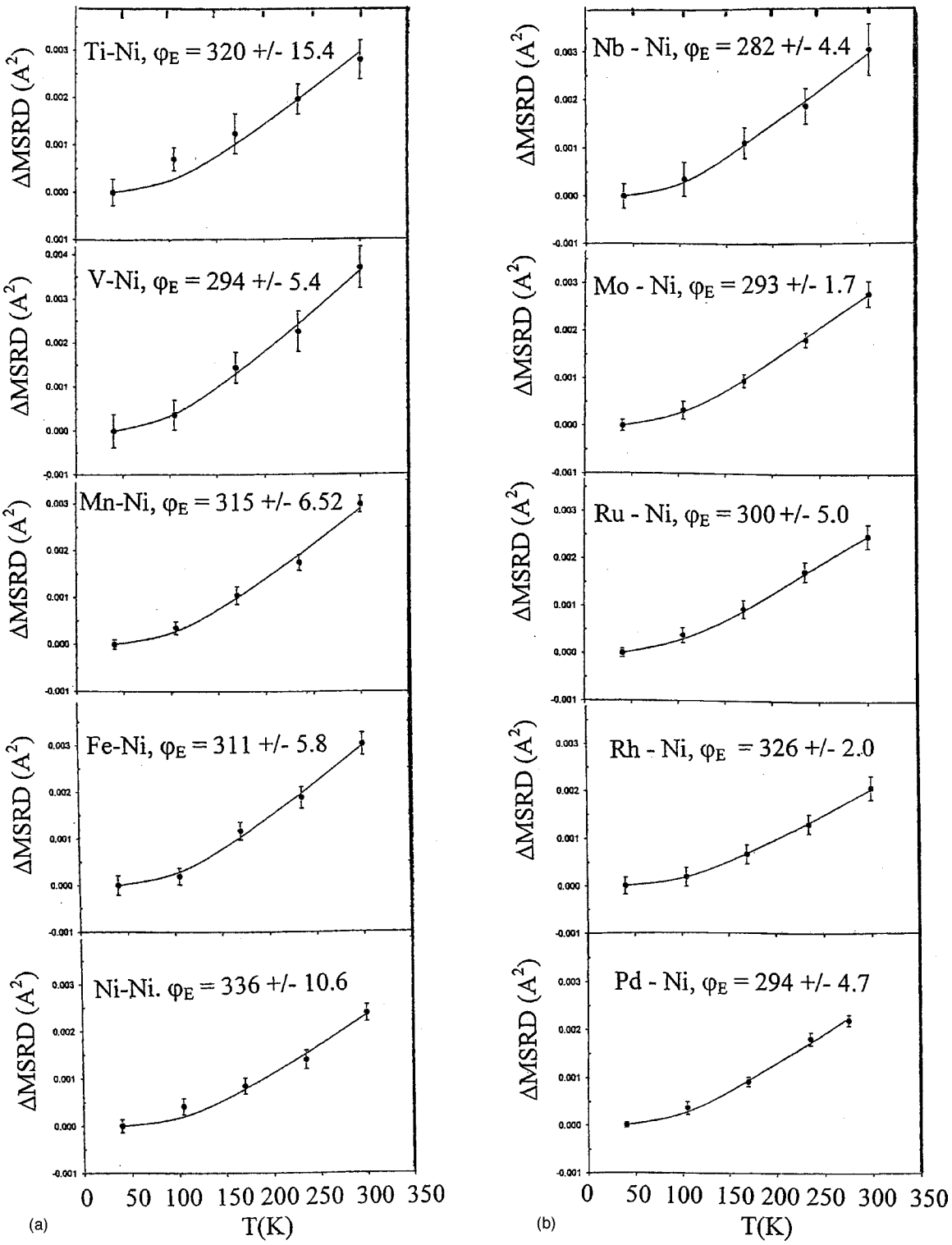

FIG. 5. Experimental ΔMSRD values versus temperature plot for (a) 3*d* dopants and (b) 4*d* dopants in Ni.

the error bars on the Einstein temperatures shown in Figs. 5(a) and 5(b), and propagating the error through Eq. (17) for r_X by standard methods.

IV. EXPERIMENTAL RESULTS AND DISCUSSION

For the 4*d* dopants in Ni, the value of r_X systematically decreases as one increases the dopant atomic number along the series Nb, Mo, Ru, and Rh, but the ratio increases sharply for Pd. Although there is no other quantitative result to which we can compare our data, we argue that the general trend we observe is reasonable. Daniel *et al.* have shown that the slope of the temperature versus the MSRD graph will be linear with shear modulus for pure fcc materials, and have also shown this relationship is true experimentally.[5] For the alloy

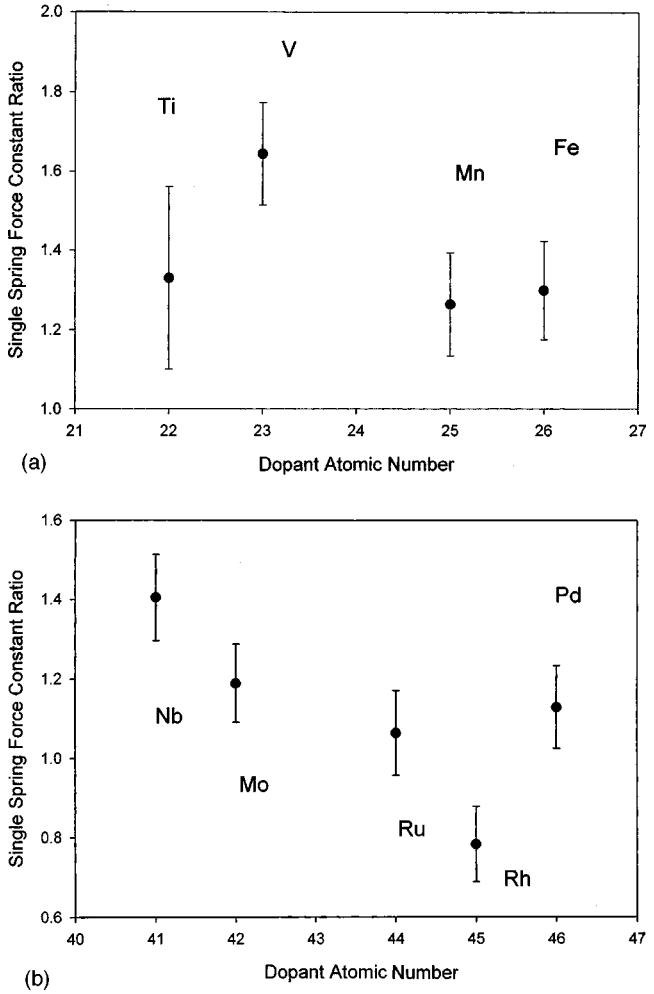

FIG. 6. Force constant ratio r_x for (a) $3d$ dopants as determined from XAFS and (b) $4d$ dopants as determined from XAFS.

case, Johnson has argued that for a solid solution of two metals having large differences in elemental atomic size, the solid solution will tend to exhibit a decreasing shear modulus with increasing supersaturation, leading to instability to formation of an amorphous phase.[17] Furthermore, even if the size difference is less than this critical value, according to Li and Johnson, fcc random solid solutions tend to exhibit decreasing local tetragonal shear modulus[18] as a dopant of large size difference is alloyed at increasing concentration into the host matrix. From our results, and those of Scheuer and Lengeler, the deviation from pure host near-neighbor distance due to doping shows a lattice expansion surrounding all the $4d$ dopants. This increase is largest for Nb dopants, where it reaches 0.07 A, and also the ratio r_X is largest for Nb dopants among the $4d$ systems we study. The local size differences observed by Scheuer and Lengeler and us drop to less than 0.02 A for Mo dopants and rises again for Pd dopants to nearly 0.06 A. However, we do not find a simple size relationship for the trends of r_X since the lattice expansion we observe for Mo, Ru, and Rh dopants are all between about 0.02 A and 0.035 A. We note that Grow *et al.* show in their review of Mossbauer results that the force constant between near neighbors in pure Mo, Nb, and Pd are significantly larger than the corresponding Fe-host force constant in the corresponding Fe doped alloy.[2] These Mossbauer findings are consistent both with our results and the size difference model of Li and Johnson[18] since doping a $4d$ host with a smaller Fe dopant, as well as doping a Ni host with a larger $4d$ dopant, should both decrease the local dopant shear resistance relative to the pure host case.

We also point out that among the $4d$ impurities studied here only Rh and Pd stabilize in the fcc structure. It is then to be noted that elemental Rh, according to band-structure calculations,[19] has the highest shear modulus among the $4d$ metals, whereas in contrast, elemental Pd has a low shear modulus about the same as copper, a noble metal.[5] The above argument is also consistent with the general trend of our data for $4d$ dopants, in that the r_X value is found to be larger for Pd than for Rh.

We next discuss relevant Mossbauer results. For the case of Fe dopants in Cu and Al hosts, recent resonant nuclear inelastic scattering results of Seto *et al.* also give force constant ratios.[20] Seto *et al.* find a value of the force constant ratio for the case of Fe in an Al host which is in disagreement with the results reported by Grow *et al.* Whereas the ratio $(1/r_X)$ reported by Grow *et al.* is 0.625, Seto *et al.* find a value of 1.1. On the other hand, the value of the force constant ratio of Fe in Cu obtained by Seto *et al.*, reproduces the corresponding data point of Grow *et al.* well.[20] With these comparisons among results obtained by different Mossbauer related methods in mind, we now consider the $3d$ dopants and compare our results for Fe dopants in Ni with the findings of Mössbauer spectroscopy. In their review, Grow *et al.* show a plot of the ratio of the impurity-host to the host-host force constant for a number of systems.[2] (Note that this ratio is the *inverse* of r_X) The only specific alloy our XAFS investigation has in common with Mössbauer studies is the system of Fe doped into Ni. There is disagreement between the Mössbauer r_X and our XAFS r_X for Fe in Ni. In the temperature range between 77 and 1345 K, Janot *et al.* find that the value of r_X is of order 0.33 to 0.5.[21] For the temperature range just above the Ni Curie temperature, Howard *et al.* find a value of r_X of $\leqslant .7$.[22] For temperature ranges from and above room temperature, Grow *et al.* find a value of r_X of $\sim 0.83 \pm 0.065$.[2] Our value of r_X, based on XAFS and the correlated Einstein model, for data taken for temperature *up to* room temperature, is 1.30. The case of Fe dopants in Ni is the one situation, amongst the systems we have studied, for which the local lattice is not expanded by the dopant. Therefore, the size difference argument cannot be used in this case to help explain the fact that our value of r_X is greater than one. Howard *et al.* state that the temperature-dependent results of Mössbauer experiments for Fe in Ni hosts may imply ''an anomalously large anharmonicity parameter in this system.'' [22]

We are certain from our XAFS results that the local environment around our Fe sites is fcc. The XAFS measurements, however, cannot rule out some kind of Fe fcc clustering, although as far as dopant near neighbors are concerned, we contend clustering is unlikely. For the Ni-rich region of the Fe-Ni phase diagram, the only ordered compound reported to tend to form is Ni_3Fe.[23] The Fe in such a compound has all Ni near neighbors. Jiang *et al.* have carried out

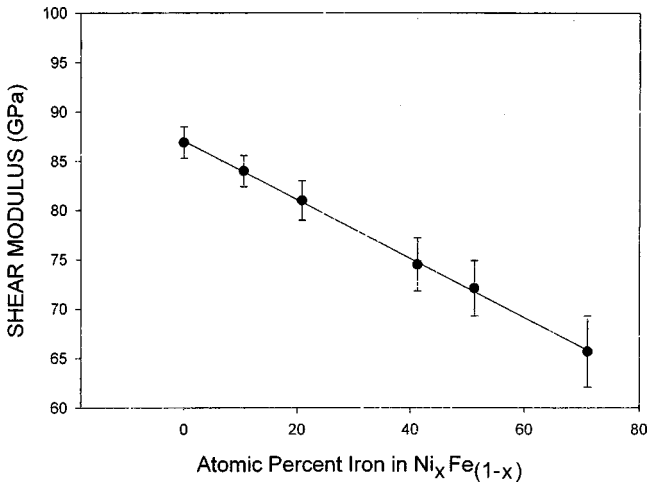

FIG. 7. Shear modulus of $Ni_xFe_{(1-x)}$ alloys as a function of x. The error bars are the upper and lower bounds determined from the Hashin-Shtrikman limits.

a thorough study of local atomic order in $Fe_{46.5}Ni_{53.5}$ and $Fe_{22.5}Ni_{77.5}$ by diffuse x-ray scattering. These samples were close to random solid solutions. Our fit result for Fe-Ni interatomic distances, 2.484(2) Å, is close to the Fe-Ni bond length obtained by Jiang *et al.*[24] (2.507 Å) for $Ni_{77.5}Fe_{22.5}$. We note that Scheuer *et al.* in their early XAFS work on dilute binary alloys obtain an Fe-Ni bond length of 2.490(3) Å.[16] This value is in excellent agreement with our Fe-Ni bond distances. On the other hand, Jiang *et al.* find that the average Fe-Fe near-neighbor distance in both alloys studied is 2.564(2) Å, significantly greater than the average Fe-Fe distance derived from the lattice spacing or the value of near-neighbor distance derived from our data. Thus, these diffuse scattering results argue against significant Fe clustering taking place in our Fe-doped Ni alloy.

There are existing elastic constant measurements for $Ni_xFe_{(1-x)}$ alloys that support our XAFS results for Fe-doped Ni, and are evidence that the Mossbauer result of an increased local force constant, for Fe dopants relative to the pure Ni case, is incorrect.[25] Single alloy crystal force constant measurements have been made for the elastic constants C_{11}, C_{12}, and C_{44}. All these force constants systematically *decrease* as the Fe concentration in the fcc Ni lattice increases. We have used these force constants to compute the upper and lower bounds on the shear modulus G for a polycrystalline alloy, using the Hashin-Shtrikman limits.[26,27] The results are plotted in Fig. 7. We do not at present have a theoretical framework to relate quantitatively our XAFS results for an alloy with the measured elastic constant data. The quantitative connection between a single spring bond strength ratio for an alloy and shear modulus of a pure material has not been explored theoretically, to our knowledge. However, Daniel *et al.* have shown an excellent correlation between shear modulus and the slope of T versus MSRD for pure fcc metals,[5] and therefore the fact that alloying with Fe systematically decreases the alloy shear modulus supports our qualitative finding that the near-neighbor single spring constant is decreased for Fe sites relative to Ni sites. The Mossbauer results, for the Fe-doped Ni system, are not supported by the elastic constant measurements.

As far as the other $3d$ dopants are concerned, with the exception of V, the force constant ratios, shown in Fig. 6(a), are about the same for different members of the $3d$ series we have studied. There is no clear picture or correlation to be drawn. In their elemental form, however, none of the $3d$ impurities stabilize in the fcc structure. We note that the ratio r_X has a sharp maximum for V impurities, and that the V impurity moment in this alloy is known to be aligned antiparallel to the host Ni magnetic moment.[28]

We feel that the use of XAFS is promising as a means to map out systematics for local impurity force constants as a function of Periodic Table position. One could search for correlations with a number of aspects of dilute alloy physics, such as virtual bound state theories, local magnetic moments, cohesive energy measurements, and atomic simulations. The on-going development of computational methods for relating MSRD results to force constants may eventually make it possible to avoid approximations such as assuming central forces, thus increasing the accuracy of the results.

On the one hand, the discrepancy between the Mossbauer and XAFS results for the case of Fe dopants in nickel might be attributable to the approximations in the correlated Einstein model used to interpret the XAFS. The theory of Mannheim used for interpreting the related Mossbauer results is the more exact theory, although neither theory takes noncentral forces into account. We also point out that the XAFS measurements are sensitive to forces parallel to the (110) direction between nearest neighbors; this might be significant if there are force anisotropies.

On the other hand, there is no straightforward way to reconcile the elastic constant measurements with the Mossbauer results. Also, one of the intriguing aspects of this topic is the dramatic temperature dependence in the force constant ratios for Fe dopants in Ni as measured by several different investigators using the Mossbauer method. The combined XAFS, elastic constant, and Mossbauer results hint at an effect such that the ratio of host-host to iron-host force constant decreases with temperature.

We consider the discrepancy between Mössbauer measurements, on the one hand, versus XAFS and elastic constant measurements, on the other hand, for the Fe doped into the Ni system to be an important aspect of this subject, an aspect which needs to be investigated further.

ACKNOWLEDGMENTS

We wish to express our appreciation for useful conversations with John Rehr and Philip Mannheim. We acknowledge the assistance of Kumi Pandya and the staff at the X-11 beam line of the National Synchrotron Light Source. This work was supported initially in part by the Department of Energy under contract number DE-FG05-94ER81861-A001, and subsequently supported by D.O.E. under contract number DE-FG05-89-ER45383.

[1] V. V. Sumin, Mater. Sci. Eng., A **230**, 63 (1997).
[2] J. M. Grow, D. G. Howard, R. H. Nussbaum, and M. Takeo, Phys. Rev. B **17**, 15 (1978).
[3] P. D. Mannheim, Phys. Rev. B **5**, 745 (1972).
[4] Nguyen Van Hung and J. J. Rehr, Phys. Rev. B **56**, 43 (1997).
[5] Million Daniel, Mahalingam Balasubramanian, Dale Brewe, Michael Mehl, Douglas Pease, and Joseph I. Budnick, Phys. Rev. B **61**, 6637 (2000).
[6] G. Beni and P. M. Platzman, Phys. Rev. B **14**, 1514 (1976).
[7] A. V. Poiarkova and J. J. Rehr, Phys. Rev. B **59**, 948 (1999).
[8] E. Sevillano, H. Meuth, and J. J. Rehr, Phys. Rev. B **20**, 4908 (1979).
[9] G. S. Knapp, H. K. Pan, and J. M. Tranquada, Phys. Rev. B **32**, 2006 (1985).
[10] N. Van Hung, N. Duc, and R. Frahm, J. Phys. Soc. Jpn. **72**, 1 (2003); **72**, 1254 (2003).
[11] L. A. Girafalco and V. G. Weizer, Phys. Rev. **114**, 687 (1959).
[12] C. A. Kittel, *Introduction to Solid State Physics*, 3rd ed. (Wiley, New York, 1998), p. 185.
[13] W. B. Pearson, *A Handbook of Lattice Spacings and Structures of Metals and Alloys* (Pergamon, New York, 1958).
[14] E. A. Stern, M. Newville, B. Ravel, and D. Haskel, Physica B **208&209**, 117 (1995).
[15] S. I. Zabinisky, J. J. Rehr, A. Ankudinov, R. C. Albers, and M. J. Eller, Phys. Rev. B **52**, 2995 (1995).
[16] U. Scheuer and B. Lengeler, Phys. Rev. B **44**, 9883 (1991).
[17] W. L. Johnson, in *Phase Transformations in Thin Films—Thermodynamics and Kinetics*, edited by M. Atzmon, A. L. Greer, J. M. E. Harper, and M. R. Libera, Mater. Res. Soc. Symp. Proc. No. 311 (Materials Research Society, Pittsburgh, 1993), p. 71.
[18] M. Li and W. Johnson, Phys. Rev. Lett. **70**, 1120 (1993).
[19] P. Söderlind, O. Eriksson, J. M. Wills, and A. M. Boring, Phys. Rev. B **48**, 5844 (1993).
[20] M. Seto, Y. Kobayashi, S. Kitao, R. Haruki, T. Mitsui, Y. Yoda, S. Nasu, and S. Kikuta, Phys. Rev. B **61**, 11 420 (2000).
[21] C. Janot and H. Scherrer, J. Phys. Chem. Solids **32**, 191 (1971).
[22] Donald G. Howard and Rudi H. Nussbaum, Phys. Rev. B **9**, 794 (1974).
[23] A. Shunk, *Constitution of Binary Alloys* (McGraw-Hill, New York, 1969).
[24] X. Jiang, G. E. Ice, C. J. Sparks, L. Robertson, and P. Zschack, Phys. Rev. B **54**, 3211 (1996).
[25] R.F.C. Hearman, *The Elastic Constants of Crystals and Other Anisotropic Materials*, Landolt-Börnstein, New Series, Group III, Vol. 18, edited by K.H. Hellwege and A.M. Hellwege (Springer-Verlag, Berlin, 1984), p. 6.
[26] Z. Hashin and S. Shtrikman, J. Mech. Phys. Solids **10**, 335 (1962).
[27] G. Simmons and H. Wang, *Single Crystal Elastic Constants and Calculated Aggregate Properties: A Handbook*, 2nd ed. (MIT, Cambridge, 1971).
[28] M. F. Collins and G. G. Low, Proc. Phys. Soc. London **86**, 535 (1965); J. Appl. Phys. **34**, 1195 (1963).